198510: mafic granulite, Mount Mackie

(*Youanmi Terrane, Yilgarn Craton*)

Blereau, ER, Kelsey, DE and Korhonen, FJ

Location and sampling

PERTH (SH 50-14), NORTHAM (2234)

MGA Zone 50, 474900E 6485500N

Warox Site FJKBGD198510

Sampled on 1 June 2010

This sample was collected from an outcrop in a field in the Avon River Valley, about 14.1 km south-southeast of the centre of Northam, 3.1 km northeast of Mount Mackie and 2.9 km west of the intersection of Wilberforce Road with Northam – York Road. The sample was collected as part of the Yilgarn Craton Metamorphic Project (2003–14) undertaken by Ben Goscombe for the Geological Survey of Western Australia (GSWA), and referred to in that study as sample BG10-5b. The results from this project have not been released by GSWA, although select data have been published in Goscombe et al. (2019). This sample is not available in the GSWA collections; all observations are based on descriptions presented in Goscombe et al. (2019) and have not been directly verified.

Geological context

The unit sampled is a mafic granulite within the shear zone system at the western margin of the Youanmi Terrane (Quentin de Gromard et al., 2021). This unit is part of a northwest-trending belt of Archean metasedimentary and gneissic rocks previously assigned to the South West Terrane and referred to informally by Wilde (2001) and Bosch et al. (1996) as the informally named Jimperding metamorphic belt. The boundary between the South West and Youanmi Terranes in this area is a major, northwest-trending shear zone system (Quentin de Gromard et al., 2021). Four quartzite samples, collected between 22 and 34 km northwest of this locality, yielded detrital zircon ages between c. 3700 and 3000 Ma, and maximum ages of deposition between c. 3203 and 3005 Ma (Wingate et al., 2008a–d; Pidgeon et al., 2010). Zircon rims in two of these samples have been interpreted to date amphibolite facies metamorphism at c. 2660 Ma (Wingate et al., 2008c,d). A pelitic migmatite sample collected about 650 m to the southwest yielded a weighted mean monazite $^{207}Pb/^{206}Pb$ date of 2664 ± 4 Ma, interpreted as the age of high-grade metamorphism (GSWA 219838; Fielding et al., 2021d). Two pelitic gneiss samples collected about 77 km to the southeast yielded weighted mean monazite $^{207}Pb/^{206}Pb$ dates of 2656 ± 6 Ma and 2651 ± 6 Ma, interpreted as the age of high-grade metamorphism (GSWA 198520, Fielding et al., 2021b; 198522, Fielding et al., 2021c). A pelitic granofels sample collected about 65 km to the southeast yielded a weighted mean monazite $^{207}Pb/^{206}Pb$ date of 2647 ± 5 Ma, interpreted as the age of high-grade metamorphism (GSWA 198516, Fielding et al., 2021a).

Petrographic description

This sample is a foliated, fine- to medium-grained, granoblastic mafic granulite containing olive green hornblende, pink–green orthopyroxene, pale green clinopyroxene, plagioclase and ilmenite (Fig. 1). Quartz and magnetite may be rare phases or absent but they have not been verified. It is unknown if the sample has undergone partial melting. Mineral compositions are provided in Table 1.

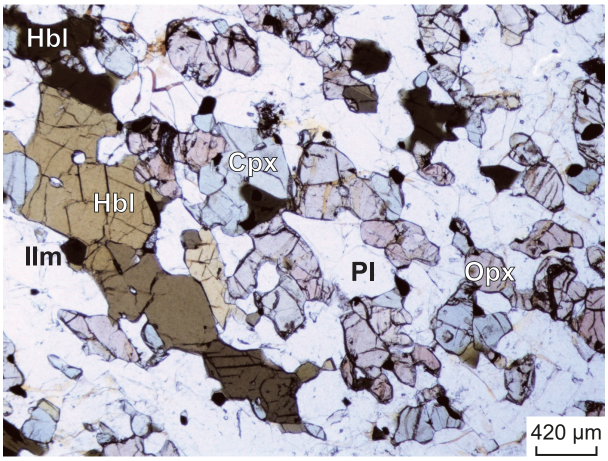

Figure 1. **Photomicrographs, in plane-polarized light, of sample 198510: mafic granulite, Mount Mackie. Mineral abbreviations are explained in the caption to Figure 2**

Table 1. Mineral compositions for sample 198510: mafic granulite, Mount Mackie

Mineral[a]	Opx	Opx	Cpx	Cpx	Ilm	Pl	Pl	Hbl	Hbl
Setting	Core	Rim	Core	Rim	Core	Core	Rim	Core	Rim
wt%									
SiO_2	50.57	50.55	51.49	51.31	0.02	54.80	54.42	42.21	42.77
TiO_2	0.10	0.10	0.24	0.18	49.84	0.01	0.01	2.48	2.43
Al_2O_3	1.08	0.97	1.95	1.74	0.00	28.95	28.72	11.15	10.86
Cr_2O_3	0.04	0.01	0.08	0.09	0.09	0.05	0.03	0.02	0.08
FeO	29.69	29.52	11.98	11.79	46.85	0.13	0.12	17.59	17.22
MnO	0.60	0.61	0.31	0.24	0.70	0.00	0.00	0.18	0.16
MgO	16.78	16.63	11.78	12.17	0.08	0.02	0.00	9.53	9.83
ZnO	0.11	0.00	0.00	0.00	0.00	0.03	0.07	0.10	0.04
CaO	0.95	0.73	22.13	21.44	0.01	11.29	11.66	11.17	11.46
Na_2O	0.02	0.00	0.38	0.36	0.00	5.00	5.00	1.72	1.61
K_2O	0.00	0.00	0.00	0.01	0.00	0.18	0.13	1.06	0.91
Total[b]	99.92	99.12	100.33	99.34	97.59	100.44	100.17	97.20	97.36
Oxygen	6	6	6	6	3	8	8	23	23
Si	1.96	1.97	1.94	1.95	0.00	2.47	2.46	6.32	6.38
Ti	0.00	0.00	0.01	0.01	0.97	0.00	0.00	0.28	0.27
Al	0.05	0.04	0.09	0.08	0.00	1.53	1.53	1.97	1.91
Cr	0.00	0.00	0.00	0.00	0.00	0.00	0.00	0.00	0.01
Fe^{3+}[c]	0.03	0.01	0.05	0.04	0.06	0.00	0.00	0.67	0.65
Fe^{2+}	0.93	0.96	0.33	0.33	0.95	0.00	0.00	1.53	1.50
Mn^{2+}	0.02	0.02	0.01	0.01	0.02	0.00	0.00	0.02	0.02
Mg	0.97	0.97	0.66	0.69	0.00	0.00	0.00	2.13	2.18
Zn	0.00	0.00	0.00	0.00	0.00	0.00	0.00	0.01	0.00
Ca	0.04	0.03	0.89	0.87	0.00	0.54	0.56	1.79	1.83
Na	0.00	0.00	0.03	0.03	0.00	0.44	0.44	0.50	0.47
K	0.00	0.00	0.00	0.00	0.00	0.01	0.01	0.20	0.17
Total	4.00	4.00	4.00	4.00	2.00	5.00	5.00	15.43	15.39
Compositional variables									
XFe[d]	0.49	0.50	0.33	0.32	–	0150	–	0.42	0.41

NOTES: – not applicable
(a) Mineral abbreviations explained in the caption to Figure 2
(b) Totals on anhydrous basis
(c) Hornblende cations calculated following Holland and Blundy (1994); Fe^{3+} contents for other minerals based on Droop (1987)
(d) $XFe = Fe^{2+}/(Fe^{2+} + Mg)$

Methodology and analytical details

Preliminary *P–T* estimates were obtained using multiple-reaction thermobarometry calculated from the mineral compositions (Table 1; Goscombe et al., 2019). These estimates were derived from the 'averagePT' module (avPT) in the program THERMOCALC version tc325 (Powell and Holland, 1988), using the internally consistent Holland and Powell (1998) dataset.

The metamorphic evolution of this sample has been subsequently re-evaluated using phase equilibria modelling, based on the bulk-rock composition (Table 2). The bulk-rock composition was determined by X-ray fluorescence spectroscopy, together with loss on ignition (LOI). The modelled O content (for Fe^{3+}) was set at 20% of the measured total Fe. A nominally anhydrous value (0.01 mole% H_2O) was chosen as the measured LOI value was negative. The bulk composition was corrected for the presence of apatite by applying a correction to CaO (Table 2). Thermodynamic calculations were performed in the NCKFMASHTO (Na_2O–CaO–K_2O–FeO–MgO–Al_2O_3–SiO_2–H_2O–TiO_2–O) system using THERMOCALC version tc340 (Powell and Holland, 1988; updated October 2013) and the internally consistent thermodynamic dataset of Green et al. (2016; version dataset tc-ds63, created January 2015). The activity–composition relations used in the modelling are detailed in Green et al. (2016), with the augite model used for clinopyroxene. Additional information on the workflow with relevant background and methodology are provided in Korhonen et al. (2020).

Table 2. Measured whole-rock and modelled compositions for sample 198510: mafic granulite, Mount Mackie

XRF whole-rock composition (wt%)[(a)]												
SiO_2	**TiO_2**	**Al_2O_3**	**Fe_2O_3[(b)]**	**FeO[(b)]**	**MnO**	**MgO**	**CaO**	**Na_2O**	**K_2O**	**P_2O_5**	**LOI**	**Total**
47.69	1.51	15.36	–	13.13	0.20	6.76	9.35	2.57	0.29	0.15	–0.18	96.82
Normalized composition used for phase equilibria modelling (mol%)												
SiO_2	**TiO_2**	**Al_2O_3**	**O[(c)]**	**FeO^{T}[(d)]**	**MnO**	**MgO**	**CaO[(e)]**	**Na_2O**	**K_2O**	**–**	**H_2O[(f)]**	**Total**
52.54	1.23	9.80	1.07	10.70	–	10.92	10.84	2.70	0.20		0.01	100

NOTES: (a) Data and analytical details are available from the WACHEM database <http://geochem.dmp.wa.gov.au/geochem/>
(b) FeO content is total Fe
(c) O content (for Fe_2O_3) set to be 20% of measured FeO[(b)]
(d) FeO^T = moles FeO + 2 * moles O
(e) CaO modified to remove apatite: CaO(Mod) = CaO(Total) - (moles CaO(in Ap) = 3.33 * moles P_2O_5)
(f) H_2O content is the measured LOI
– not applicable

Results

The *P–T* pseudosection for sample 198510 was calculated over a temperature range of 3–8 kbar and 750–900 °C (Fig. 2). The solidus is located between 780 and 870 °C across the range of modelled pressures. Magnetite is stable at low pressure below about 6 kbar, quartz is stable at higher pressures above 6 kbar across the range of modelled temperatures and K-feldspar is stable below 825 °C across the modelled pressures. Biotite is stable at temperature lower than about 850 °C and pressure less than about 6.6 kbar at 750 °C (Fig. 2).

Metamorphic *P–T* estimates (± 2σ uncertainty) calculated using multiple-reaction thermobarometry are 5.5 ± 2.0 kbar and 820 ± 61 °C (Goscombe et al., 2019). These calculations used the mineral core compositions (Table 1) to estimate peak conditions. Conventional thermobarometry using the orthopyroxene–clinopyroxene thermometer reportedly yield results of 790–800 °C and 800–830 °C, presumably from rims and cores, and the Al-in-hornblende barometer yields 5.9 kbar (Goscombe et al., 2019).

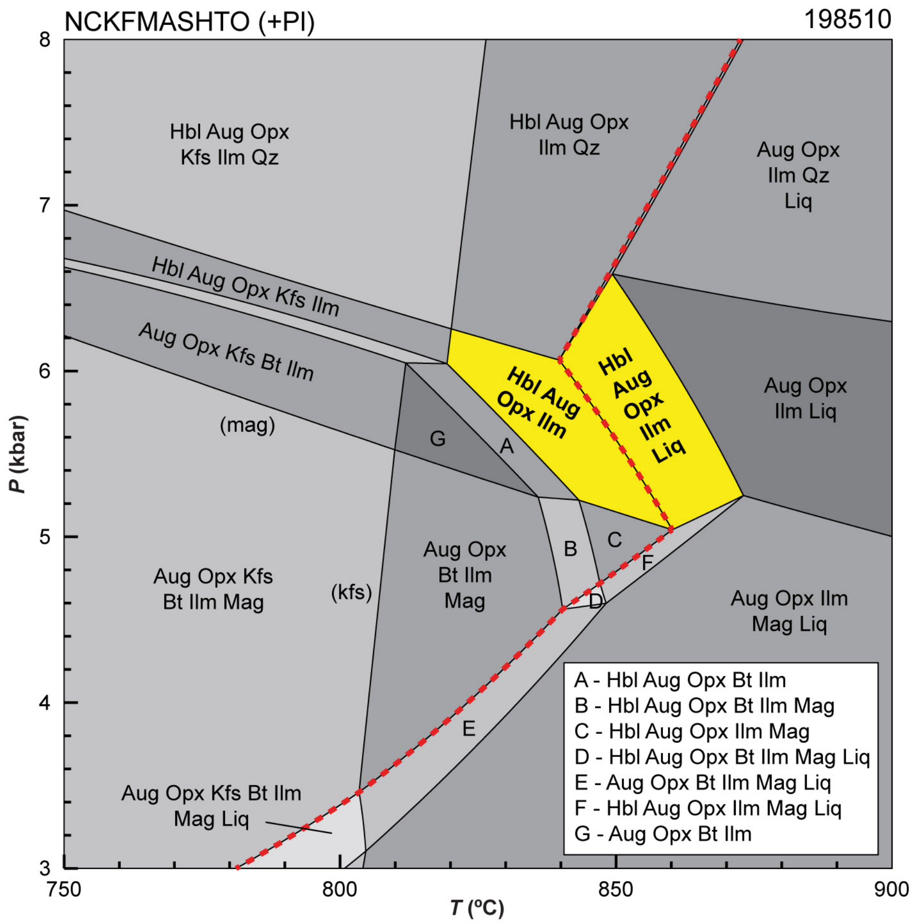

Figure 2. ***P–T*** **pseudosection calculated for sample 198510: mafic granulite, Mount Mackie. Assemblage fields corresponding to peak metamorphic conditions are shown in bold text and yellow shading. Red dashed line represents the solidus. Abbreviations: Aug, augite; Bt, biotite; H_2O, fluid (pure H_2O); Hbl, hornblende; Ilm, ilmenite; Kfs, K-feldspar; Liq, silicate melt; Mag, magnetite; Opx, orthopyroxene; Pl, plagioclase; Qz, quartz**

Interpretation

The interpreted peak metamorphic assemblage of hornblende–clinopyroxene–orthopyroxene–plagioclase–ilmenite(–melt) is stable between 820 and 875 °C at 5.0 – 6.6 kbar, as shown by the yellow-coloured fields in Figure 2. There is uncertainty whether the rock has undergone partial melting and whether it contains magnetite and quartz. In the absence of information about them the conservative constraint on the peak *P–T* conditions excludes both these minerals (Fig. 2). Within uncertainty the results determined from multiple-reaction thermobarometry overlap with the peak hornblende–clinopyroxene–orthopyroxene–plagioclase–ilmenite field. There is no information on the prograde and retrograde segments of the *P–T* path, and therefore it is not possible to constrain the overall shape of the *P–T* path.

Peak metamorphic conditions are estimated at 820–875 °C and 5.0 – 6.6 kbar, with an apparent thermal gradient between 130 and 170 °C/kbar.

References

Bosch, D, Bruguier, O and Pidgeon, RT 1996, Evolution of an Archean metamorphic belt: A conventional and SHRIMP U–Pb study of accessory minerals from the Jimperding metamorphic belt, Yilgarn Craton, Western Australia: The Journal of Geology, v. 104, p. 695–711.

Droop, GTR 1987, A general equation for estimating Fe^{3+} concentrations in ferromagnesian silicates and oxides from microprobe analyses, using stoichiometric criteria: Mineralogical Magazine, v. 51, no. 361, p. 431–435.

Fielding, IOH, Wingate, MTD, Korhonen, FJ and Rankenburg, K 2021a, 198516: pelitic granofels, Quajabin Peak; Geochronology Record 1764: Geological Survey of Western Australia, 5p.

Fielding, IOH, Wingate, MTD, Korhonen, FJ and Rankenburg, K 2021b, 198520: pelitic granofels, Tregenza Road; Geochronology Record 1765: Geological Survey of Western Australia, 5p.

Fielding, IOH, Wingate, MTD, Korhonen, FJ and Rankenburg, K, 2021c; 198522: pelitic granofels, Tregenza Road; Geochron Record 1766: Geological Survey of Western Australia, 5p.

Fielding, IOH, Wingate, MTD, Korhonen, FJ and Rankenburg, K 2021d, 219838: granitic gneiss, Mount Mackie; Geochronology Record 1772: Geological Survey of Western Australia, 5p.

Goscombe, B, Foster, DA, Blewett, R, Czarnota, K, Wade, B, Groenewald, B and Gray, D 2019, Neoarchaean metamorphic evolution of the Yilgarn Craton: a record of subduction, accretion, extension and lithospheric delamination: Precambrian Research, v. 335, article no. 105441, doi:10.1016/j.precamres.2019.105441.

Green, ECR, White, RW, Diener, JFA, Powell, R, Holland, TJB and Palin, RM 2016, Activity–composition relations for the calculation of partial melting equilibria in metabasic rocks: Journal of Metamorphic Geology, v. 34, no. 9, p. 845–869.

Holland, T and Blundy, J 1994, Non-ideal interactions in calcic amphiboles and their bearing on amphibole-plagioclase thermometry: Contributions to Mineralogy and Petrology, v. 116, no. 4, p. 433–447.

Holland, TJB and Powell, R 1998, An internally consistent thermodynamic data set for phases of petrological interest: Journal of Metamorphic Geology, v. 16, no. 3, p. 309–343.

Korhonen, FJ, Kelsey, DE, Fielding, IOH and Romano, SS 2020, The utility of the metamorphic rock record: constraining the pressure–temperature–time conditions of metamorphism: Geological Survey of Western Australia, Record 2020/14, 24p.

Pidgeon, RT, Wingate, MTD, Bodorkos, S and Nelson, DR 2010, The age distribution of detrital zircons in quartzites from the Toodyay– Lake Grace Domain, Western Australia: implications for the early evolution of the Yilgarn Craton: American Journal of Science, v. 310, p. 1115–1135.

Powell, R and Holland, TJB 1988, An internally consistent dataset with uncertainties and correlations: 3. Applications to geobarometry, worked examples and a computer program: Journal of Metamorphic Geology, v. 6, no. 2, p. 173–204.

Quentin de Gromard, R, Ivanic, TJ and Zibra, I 2021, Pre-Mesozoic Interpreted Bedrock Geology of the southwest Yilgarn, 2021: Geological Survey of Western Australia, digital data layer, < www.dmirs.wa.gov.au/geoview>.

Wilde, SA 2001, Jimperding and Chittering metamorphic belts, Western Australia— a field guide: Geological Survey of Western Australia, Record 2001/12, 24p.

Wingate, MTD, Bodorkos, S, and Kirkland, CL 2008a, 177901: quartzite, Kowalyou; Geochronology Record 739: Geological Survey of Western Australia, 5p.

Wingate, MTD, Bodorkos, S, and Kirkland, CL 2008b, 177904: quartzite, Windmill Hill; Geochronology Record 740: Geological Survey of Western Australia, 7p.

Wingate, MTD, Bodorkos, S, and Kirkland, CL 2008c, 177907: quartzite, Noondeening Hill; Geochronology Record 741: Geological Survey of Western Australia, 7p.

Wingate, MTD, Bodorkos, S, and Kirkland, CL 2008d, 177908: quartzite, Noondeening Hill; Geochronology Record 742: Geological Survey of Western Australia, 7p.

Links

Metamorphic history introduction document: Intro_2020.pdf

Recommended reference for this publication

Blereau, ER, Kelsey, DE and Korhonen, FJ 2021, 198510: mafic granulite, Mount Mackie; Metamorphic History Record 7: Geological Survey of Western Australia, 6p.

Data obtained: 19 May 2020

Date released: 25 June 2021

This Metamorphic History Record was last modified on 9 June 2021.

Grid references in this publication refer to the Geocentric Datum of Australia 1994 (GDA94). All locations are quoted to at least the nearest 100 m.

WAROX is GSWA’s field observation and sample database. WAROX site IDs have the format ‘ABCXXXnnnnnnSS’, where ABC = geologist username, XXX = project or map code, nnnnnn = 6 digit site number, and SS = optional alphabetic suffix (maximum 2 characters).

Isotope and element analyses are routinely conducted using the GeoHistory laser ablation ICP-MS and Sensitive High-Resolution Ion Microprobe (SHRIMP) ion microprobe facilities at the John de Laeter Centre (JdLC), Curtin University, with the financial support of the Australian Research Council and AuScope National Collaborative Research Infrastructure Strategy (NCRIS). The TESCAN Integrated Mineral Analyser (TIMA) instrument was funded by a grant from the Australian Research Council (LE140100150) and is operated by the JdLC with the support of the Geological Survey of Western Australia, The University of Western Australia (UWA) and Murdoch University. Mineral analyses are routinely obtained using the electron probe microanalyser (EPMA) facilities at the Centre for Microscopy, Characterisation and Analysis at UWA, and at Adelaide Microscopy, University of Adelaide.

Digital data related to WA Geology Online, including geochronology and digital geology, are available online at the Department’s Data and Software Centre and may be viewed in map context at GeoVIEW.WA.

Further details of geoscience products are available from:
Information Centre
Department of Mines, Industry Regulation and Safety
100 Plain Street
EAST PERTH WA 6004
Telephone: +61 8 9222 3459 | Email: publications@dmirs.wa.gov.au
www.dmirs.wa.gov.au/GSWApublications